Chapter 2
Quantitative Analysis for p53 Tetramerization Domain Mutants Reveals a Low Threshold for Tumor Suppressor Inactivation

2.1 Introduction

Genome instability and DNA breakage are the hallmarks of cancer cells that arise in response to the activation of oncogenes through point mutations, gene amplifications, or gene translocations [1, 2]. Counterbalancing the effects of oncoproteins are tumor suppressor proteins, the most important of which is p53, a transcription factor that modulates cell cycle arrest, senescence, apoptosis, and DNA repair largely via the direct or indirect induction or repression of hundreds of genes [3].

The p53 tumor suppressor monomer is a 393 amino acid protein with five domains: An N-terminal transactivation domain (91–42); a proline- rich domain (61–92); a central site-specific DNA-binding domain (101–300); a tetramerization domain (TD, 326–356); and a C-terminal basic domain (364–393). Several stressors, including DNA damage, activate p53 partly through multiple post-translational modifications modulating its activity and stability [4]. However, wild-type p53 acts as a transcription factor only when it binds site-specific DNA response elements as a tetramer [5]. Furthermore, a number of the post-translational modifications that are believed to be important regulators of p53 activity depend on its quaternary structure [6–11]. The p53 protein also exhibits transcription-independent apoptogenesis, possibly contributing to its role in tumor suppression, that is mediated through its interaction with BCL2 family members, including Bak. The efficient targeting to and oligomerization of Bak in the mitochondrial membrane reportedly depends on p53 oligomerization [12]. Thus, tetramer formation by p53 is crucial to its tumor suppressive activity.

About half of human tumors carry inactivating mutations in the *TP53* gene [13, 14]. Unlike other tumor suppressor genes, such as *RB1*, *APC*, *BRCA1*, and *CDKN2A* that are inactivated primarily by deletion or nonsense mutations, 74% of *TP53* tumor-derived mutations are point mutations that change a single amino acid. More than 95 % of these missense mutations occur in the DNA-binding

R. Kamada, *Tetramer Stability and Functional Regulation of Tumor Suppressor Protein p53*, Springer Theses, DOI: 10.1007/978-4-431-54135-6_2,

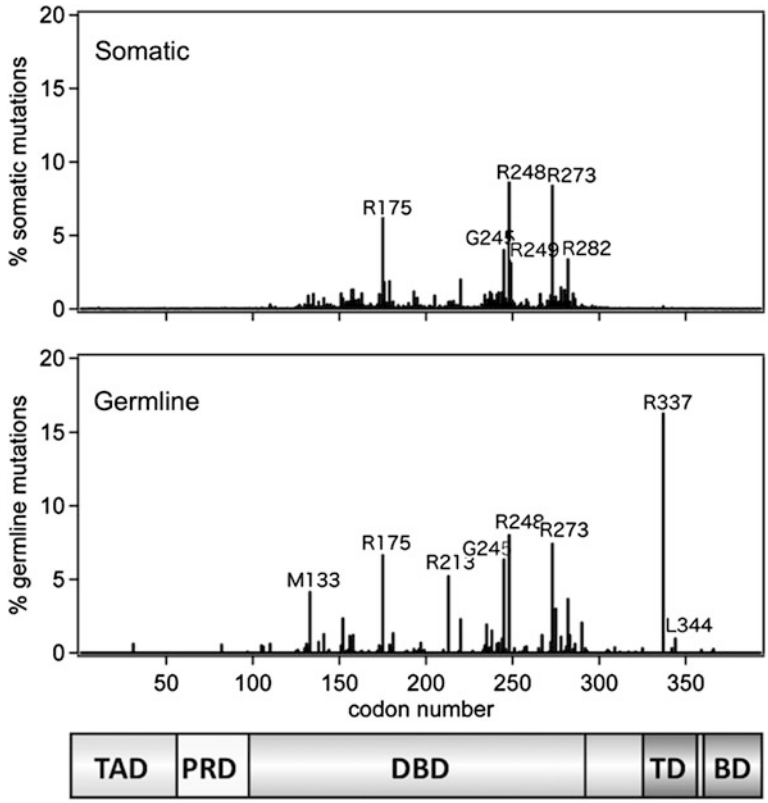

Fig. 2.1 Relative frequency of somatic (*top*) and germline (*bottom*) mutations along p53 sequence. Codon 337 in the tetramerization domain is the most frequently affected position in p53 germline mutations. From the IARC TP53 Mutation Database, release R14, November 2009)

domain; they fall into two main categories, commonly termed DNA contact- and conformational-mutations (Fig. 2.1). In contrast, about 17 % of germ-line p53 mutations in people with Li-Fraumeni syndrome and Li-Fraumeni-like ones affect amino acids in the TD even though it consists only of a short amino acid segment ($\approx$30 a.a.), while $\sim$80 % of germ-line mutations affect DNA-binding domain residues, viz., six times as long as the TD [14]. This finding implies that germ-line mutations exist at similar frequencies in the tetramerization and DNA-binding domains, and both are essential for p53-mediated tumor suppressor activity.

The p53TD consists of a β-strand (Glu326-Arg333), a tight turn (Gly334), and an α-helix (Arg335-Gly356) [15]. The structure of the TD was determined by NMR spectroscopy [16] and *X*-ray crystallography [17]. Two monomers form a dimer through their antiparallel β-sheets and α-helices, and two dimers become a tetramer through the formation of an unusual four-helix bundle. Alanine (Ala)-scanning of p53TD revealed that nine hydrophobic residues constitute critical determinants of its stability and oligomerization status [18]. An earlier study of

tumor-derived mutants R337C, R337H, and L344P from patients with Li-Fraumeni-like syndrome revealed a propensity for dramatic destabilization; the presence of the R337H mutation entailed pH-dependent instability of the mutant p53 tetramer [19]. Leu344 occurs in the α-helix, and after introducing a helix-breaking proline (L344P), p53 could not form tetramers. R337C forms dimers and tetramers at low temperature; however, even though its tetrameric structure is destabilized significantly at physiological temperatures, it is only partially inactivated in several functional assays [20, 21]. The p53 proteins with these mutations, as with other p53TD mutations (e.g., L330H, R337L, R342P, E349D and G334V), exhibit an overall decrease in DNA-binding and transactivation activity [22, 23].

Because the p53 tetramer is in equilibrium with the monomer, the protein concentration of p53 will affect its oligomeric status [18, 24]. In unstressed normal cells, p53 is maintained at low levels by continuous ubiquitylation and subsequent degradation by the 26S proteasome [25]. DNA damage-induced phosphorylation of N-terminal residues of p53, and of Mdm2, an ubiquitin protein ligase, inhibits its binding to the latter and enables p53 stabilization and accumulation [4]. A high concentration of p53 shifts the monomer-tetramer equilibrium toward the tetramer state, thereby promoting increased DNA binding and interactions with proteins important for p53 activation and function, and heightening post-translational modifications that activate p53. Past research used only semi-quantitative analyses to assess the effects of mutations on the oligomeric structure and transcriptional activity of p53 [26–28]. Whilst this research determined the oligomeric status of the mutant p53 protein by cross-linking [27] or by Fluorescence Intensity Distribution Analysis (FIDA) [28], the abundance of the p53 protein was not controlled; thus, a destabilized mutant might show wild-type stability under high concentrations of mutant p53.

In this study, I quantitatively analyzed the oligomeric structure and stability of TD peptides from the reported cancer-associated, TD mutants of p53. Surprisingly, the abilities of these mutants to form tetramers spanned a broad, almost continuous distribution. While mutants that changed the domain core drastically prevented tetramer formation and/or folding as previously reported, the effects of many mutants were much more subtle. Nevertheless, even for mutants that slightly destabilized tetramer formation, at an endogenous concentration of p53, the fraction of tetramer is significantly decreased. The data further suggested that additional studies of the biochemical and biophysical properties of the TD might be required to explain why some p53 TD mutations are cancer-associated.

2.2 Experimental Procedures

2.2.1 Peptide Synthesis and Purification

WT- and mutant-p53TD peptides, comprising residues 319–358 of the extended TD, were synthesized as described previously [29]. Peptide concentrations were measured spectrophotometrically using an extinction coefficient for mutant p53TD

peptides, $\varepsilon_{280} = 1280\ M^{-1}\ cm^{-1}$, corresponding to a single tyrosine; for G334W and G356W, $\varepsilon_{280} = 6800\ M^{-1}\ cm^{-1}$, corresponding to a single tyrosine and a tryptophan. Because the peptides Y327D, Y327H, and Y327S have no Tyr or Trp, peptide concentrations were determined by the BCA method (Pierce Co.) using a WT peptide as the standard.

2.2.2 Gel Filtration Chromatography

The WT- and mutant-p53TD peptides were resolved using a Superdex 75 PC 3.2/30 (GE Healthcare) with a Precision Column Holder (GE Health) in 50 mM phosphate buffer pH 7.5, 100 mM NaCl [29]. Peptide concentrations were 100 μM. The flow-rate was 0.1 mL/min at 15 °C, and the effluent at 214 nm was monitored. Each peak was quantified by calculating the peak area using IGOR software (Wavemetrics).

2.2.3 Thermal Denaturation by Circular Dichroism Spectroscopy

For the CD measurements, a Jasco-805 spectropolarimeter was employed using a 1 mm path-length quartz cell. CD spectra were recorded in 50 mM sodium phosphate buffer containing 100 mM NaCl, pH 7.5. For the thermal denaturation studies, spectra were recorded at discrete temperatures from 4 to 96 °C with a scan rate of 1 °C/min; ellipticity was measured at 222 nm for the p53TD solutions (10 μM monomer in 50 mM phosphate buffer, pH 7.5). The unfolding process of the p53TD peptide was fitted to a two-state transition model wherein the native tetramer directly converts to an unfolded monomer, as previously described [18, 24]. The thermodynamic parameters of the peptides were determined by calculation with the functions described by Mateu et al. [18]. The T_m and ΔH^{Tm} was determined by fitting the fraction of monomer; we estimated the K_d value of the tetramer-monomer transition from $K_d = ((1-K_u)/2)^{-1/3}$ [30]. For dimer mutants, $K_d = K_u^{-1}$ was used. The oligomeric states at 37 °C against the peptide concentration were assessed via the K_d value.

2.2.4 Structural Modeling of p53TD Mutants

The three-dimensional coordinates of p53TD wild-type (PDB: 3sak) were used as a template. Homology modeling of mutants was performed with Modeller software [31].

Table 2.1 Missense mutations found in tetramerization domain

mutation			tumor type		mutation			tumor type
Glu	326	Gly	Skin	β-strand	Arg	337	Pro	Breast, Lung, Ovary
Tyr	327	Asp	Colorectum		Phe	338	Ile	Breast
		His	Skin				Leu	Adrenal Gland
		Ser	Breast		Glu	339	Gln	Breast
Phe	328	Leu	Skin				Lys	Head and Neck
		Ser	Colorectum		Phe	341	Cys	Breast, Prostate Gland
		Val	Stomach		Arg	342	Gln	Larynx, Prostate Gland
Thr	329	Ile	Head and Neck				Leu	Brain
		Ser	Ovary				Pro	Breast, Ovary
Leu	330	Arg	Breast		Glu	343	Gly	Colon, Lung
		His	Liver, Ovary		Leu	344	Arg	Bladder
		Pro	Colorectum				Pro	Hypopharynx
Gln	331	Arg	Prostate Gland		Glu	346	Ala	Nasopharynx
		His	Breast, Lung		Ala	347	Gly	Brain
		Pro	Esophagus				Thr	Lung, Breast, Ovary
Ile	332	Val	Ovary		Leu	348	Phe	Lung
Gly	334	Trp	Lung	turn			Ser	Oropharynx
		Val	Lung		Glu	349	Asp	Bladder
Arg	335	Gly	Pancreas	α-helix	Lys	351	Asn	Ovary
		His	Lung		Asp	352	His	Esophagus
		Leu	Other and Unspecified Parts of Mouth		Ala	353	Thr	Bladder
					Gln	354	Arg	Kidney
Arg	337	Cys	Bones, Brain, Breast, Colorectum, Esophagus				Glu	Lymph Nodes
							Lys	Head and Neck
		His	Adrenal Gland, Liver		Gly	356	Ala	Pancreas
		Leu	Breast, Prostate Gland				Trp	Corpus Uteri, Vulva

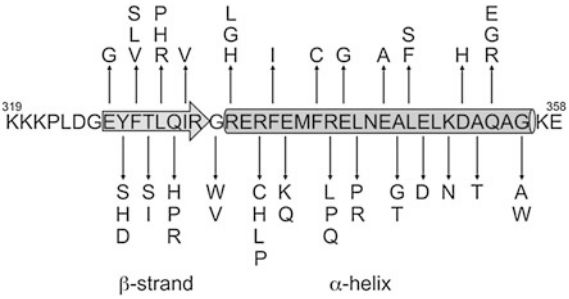

Fig. 2.2 Amino acid sequences and the positions of the missense mutations in the TD of p53. Forty-nine distinct mutations were reported in 23 residues among 31 residues of the tetramerization domain

2.3 Results

2.3.1 Oligomerization State of Mutant p53 Tetramerization Domains

Fifty distinct mutations in human cancers occur in 25 of the 31 residues that comprise the p53 core TD (amino acids 326–356) (Table 2.1, Figs. 2.2, 2.3). Wild-type (WT) and mutant p53TD peptides corresponding to residues 319–358 were synthesized and their oligomeric state and thermodynamic stability were analyzed; I quantified this state from the peak areas corresponding to a monomer and tetramer during gel-filtration chromatography (Table 2.2). WT and most

Table 2.2 The fraction of tetramer determined by gel filtration chromatography

No.	mutant	State	Tetramer (%)	No.	mutant	State	Tetramer (%)
	WT	M-T	90.7	26	F338I	M-T	65.9
1	E326G	M-T	87.8	27	F338L	M-T	75.2
2	Y327D	M-T	85.0	28	E339 K	M-T	83.2
3	Y327H	M-T	87.1	29	E339Q	M-T	84.0
4	Y327S	M-T	81.1	30	F341C	M-D	55.4*
5	F328L	M-T	88.2	31	R342L	M-T	90.4
6	F328S	M-T	74.4	32	R342P	M	0.0
7	F328 V	M-T	83.5	33	R342Q	M-T	88.8
8	T329I	M-T	84.5	34	E343G	M-T	78.1
9	T329S	M-T	89.7	35	L344P	M	0.0
10	L330H	M-T	45.1	36	L344R	M-D	61.0*
11	L330P	M	0.0	37	E346A	M-T	81.4
12	L330R	M	0.0	38	A347G	M-T	88.3
13	Q331H	M-T	85.6	39	A347T	M-D	62.1[a]
14	Q331P	M-T	88.4	40	L348F	M-T	76.3
15	Q331R	M-T	90.9	41	L348S	M-T	40.5
16	I332 V	M-T	88.5	42	E349D	M-T	89.5
17	G334 V	M-T-A	84.3	43	K351 N	n.d.	n.d.
18	G334 W	M-T	82.0	44	D352H	M-T	89.7
19	R335G	M-T	62.2	45	A353T	M-T	76.9
20	R335H	M-T	89.5	46	Q354E	M-T	85.2
21	R335L	M-T	81.3	47	Q354 K	M-T	82.2
22	R337C	M-T-A	54.8	48	Q354R	M-T	85.7
23	R337H	M-T	80.9	49	G356A	M-T	91.2
24	R337L	M-T	80.4	50	G356 W	M-T	88.6
25	R337P	M	0.0				

M-T, Monomer-Tetramer; M-D, Monomer–Dimer; M-T-A, Monomer-Tetramer-Aggregate
[a] Fraction of dimer; n.d., not determined

mutant peptides eluted as tetramers, but five, L330P, L330R, R337P, L342P, and L344P, eluted as a single peak contemporaneously with the monomer mutant L330A. Interestingly, three mutants (F341C, L344R, and A347T) eluted between the tetramer and monomer fractions. Accordingly, five mutants, L330R/P, R337P, L342P, and L344P, exist as monomers, three mutants, F341C, L344R, and A347T as dimers, and the others as tetramers under conditions used in this study. Moreover, some mutants, such as L330H, R337C, and L348S, contained a lower tetramer fraction (45.1, 54.8, and 40.5 %, respectively), and part of these peptides chromatographed as monomers, implying destabilization of their tetrameric structure, thus favoring the monomer side of the monomer-tetramer equilibrium.

2.3.2 Secondary Structure of Mutant p53 Tetramerization Domains

The secondary structures of all mutant peptides were deduced from their CD spectra (Fig. 2.3). Five monomeric mutants (L330P, L330R, R337P, R342P, and L344P) showed a negative minimum near 200 nm, characteristic of a random coil, even under a high (10 μM) peptide concentration and low temperature of 4 °C. Seemingly, substitutions by Pro catastrophically affect tetramer formation. Five mutants (L330H, Q331P, R337C, F338I, and L348S) showed weaker negative CD spectra between ~210 and 240 nm compared with the WT, pointing to destabilized WT-like tetrameric structures. The three dimer mutants (F341C, L344R, and A347T) displayed the same spectra as the other tetrameric mutants, indicating that their α-helical segment and *β*-strand are structurally similar to those of the WT tetramer. Still other mutant peptides formed WT-like tetrameric structures under these same conditions.

2.3.3 Thermal Stability of the Mutant p53 Tetramerization Domains

The effects of temperature on the conformation of the WT and mutant peptides were analyzed by calculating the thermal denaturation curves for each p53 peptide from changes in CD ellipticity at 222 nm, using a two-state transition mode. Figures 2.4, 2.5 and Table 2.3 show that the effects of amino acid changes on the tetramer's stability elicited alterations in the ΔT_ms of the mutant peptides from 4.8 to −46.8 °C. Changes to the TD hydrophobic core residues (F328, L330, R337, F338, F341, L344, and L348), except for I332V, dramatically lowered stability; modifications to solvent-exposed residues had less profound effects. The introduction of proline into the α-helix (R337P, R342P, and L344P) devastated tetramer formation; these peptides existed substantially as monomers only. No cancer-associated mutation has been reported in the codon for the hydrophobic core residue Met340. Four cancer-associated mutants changed amino acids such as to actually increase tetramer stability (T329I, Q331H, Q331R, and G356A; Table 2.3, Fig. 2.4). I noted a good correlation between the fraction of oligomers analyzed by gel filtration and the T_m value of the mutants obtained by CD (Fig. 2.11), indicating that these thermodynamic parameters corresponded to the tetrameric state of the p53 peptides.

2.3.4 Effects of Mutation on the Tetrameric Structure

Especially, Pro mutations in the α-helix caused devastating effects on tetramer formation and these peptides existed only as the monomer (Fig. 2.3). Mutations of

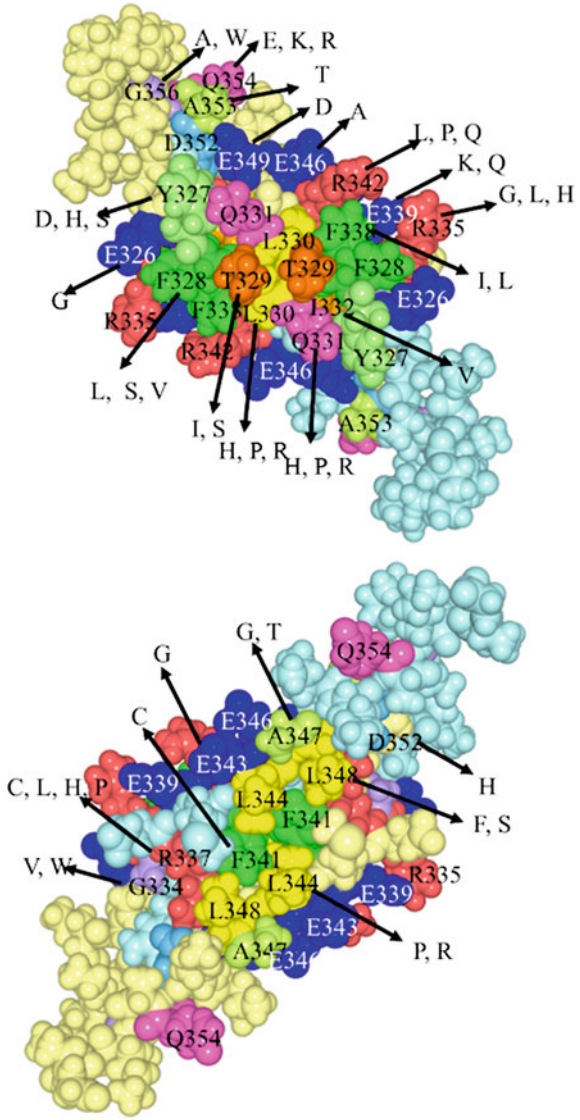

Fig. 2.3 Space-filling model of p53TD (pdb; 3sak) prepared with MolFeat version 4.0 (FiatLux Corp.) The amino acid residues of the mutation site in the p53TD and the location of these residues in the tetrameric structure are shown. The primary dimers are depicted, and the other dimer is removed to give a direct view of the protein's interior. The bottom dimer was obtained by rotating the structure in the top picture by 180° around the vertical axis

amino acid residues in the hydrophobic core of the p53 tetramerization domain induced dramatic reduction in stability of the structures. On the other hand, mutations of the residues accessible to solvent were less effective in destabilizing the tetrameric structures. Interestingly, the stability of the mutants was highly dispersed and there was no large stability gap between the mutants. These results suggested that similar to the case of the mutations (R337H, L344P) found in Li-Fraumeni syndrome, other mutations cause destabilization of the tetrameric structure and are associated with dysfunction of the tumor suppressor activity of

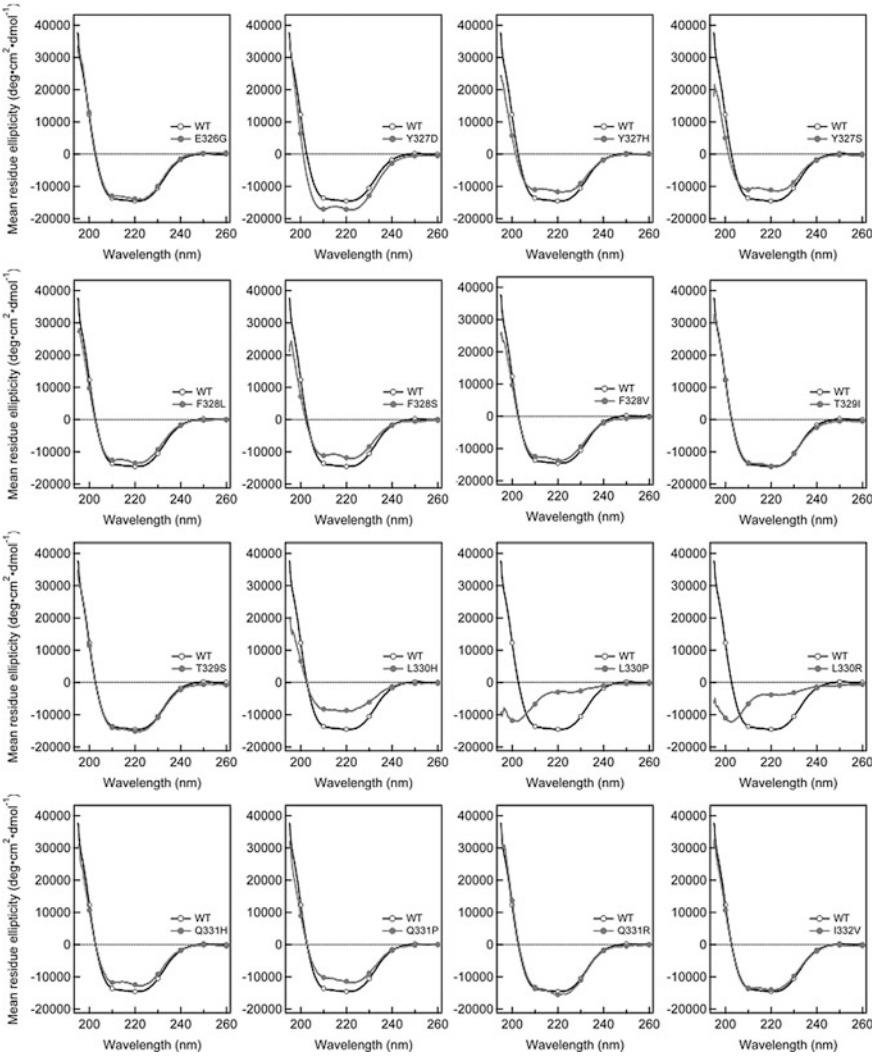

Fig. 2.4 CD spectra of WT and mutant p53TD peptides. CD spectra of WT and mutant p53TD peptides in 50 mM phosphate buffer, pH 7.5, 100 mM NaCl at 4 °C. Peptide concentration was 10 μM

p53 protein. Thus, the threshold resulting in destabilization of the structure and hence loss of p53 tumor suppressor function could be extremely low.

Three mutants (F341C, L344R, and A347T), which formed dimers, were strongly destabilized (T_m = 23.8–44.3 °C) (Fig. 2.6). F341C was the most destabilized mutant out of the three (T_m = 23.8 °C). Phe341 is located in the hydrophobic core and the hydrophobicity of the Phe residue stabilized the tetrameric structure of p53. The Phe341 residue from one peptide chain is located near another Phe341 residue

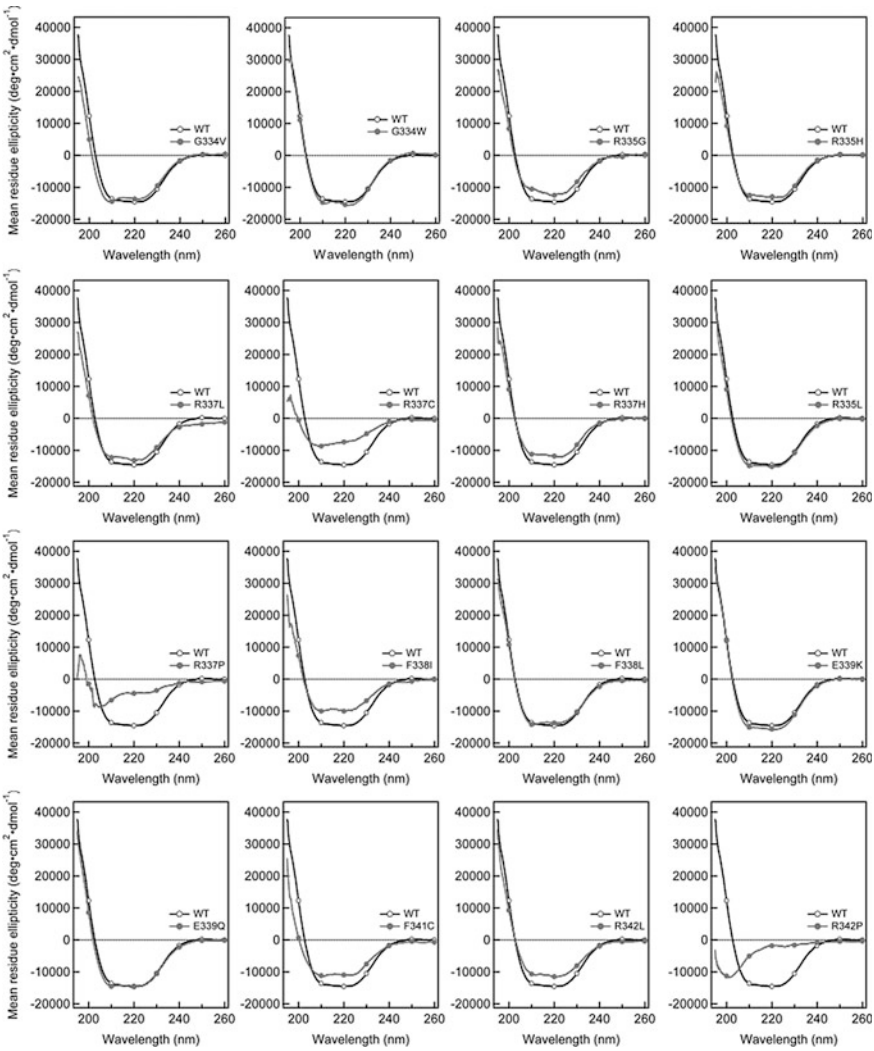

Fig. 2.4 continued

from the opposite side-chain. The mutation of Phe341 to Cys might result in the ability of C341 to form a disulfide bond in the tetrameric structure. Leu344 and Ala347 are located at the dimer–dimer interface, and Leu344 also constitutes part of the hydrophobic core of the tetramer. It is clear that mutation of Leu344 to Arg resulting in a charged polar side chain disrupts the tetrameric structure of p53. The Ala347 residue from one peptide chain and a residue from another peptide chain are in an opposite position. A347G could form tetramers although its stability was moderately destabilized. In contrast, A347T could not form tetramers because of the substitution with Thr, which has a more bulky side chain than Gly.

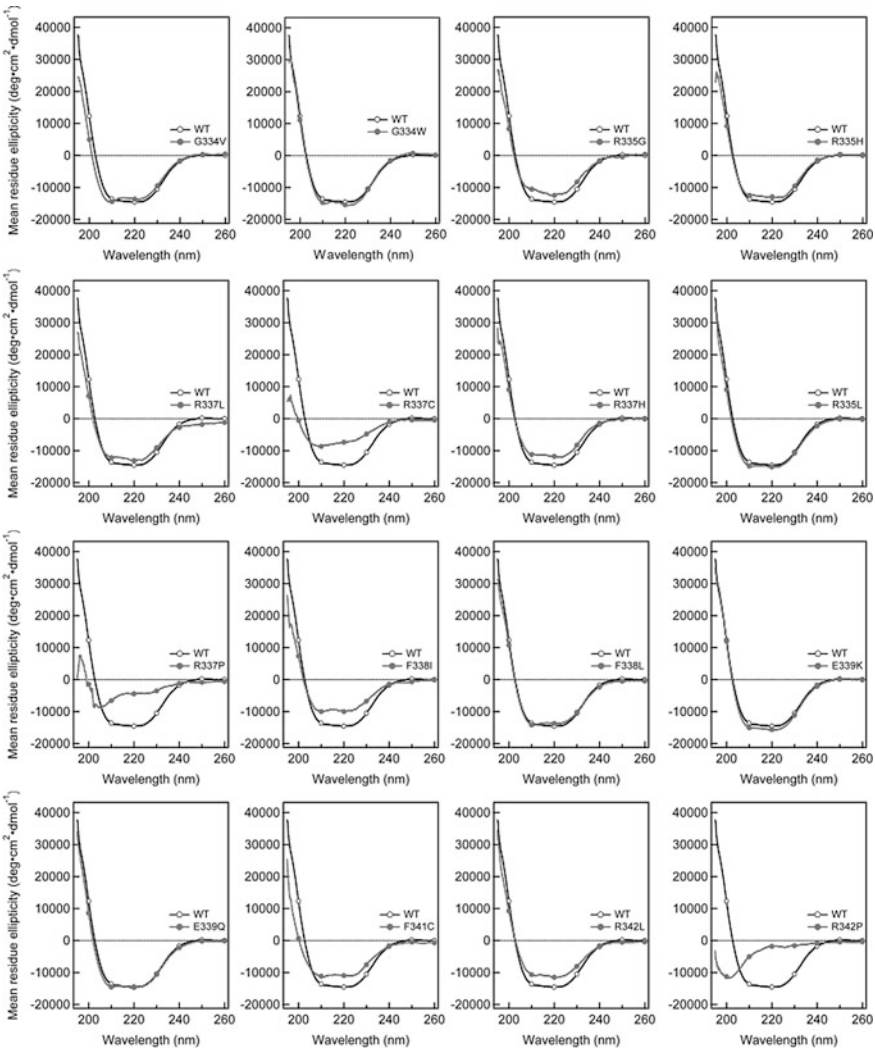

Fig. 2.4 continued

Ten mutant peptides (F328V, F328S, L330H, G334V, R335G, R337C, R337L, R337H, F338I, and L348S) formed tetramers at 10 μM concentration of the monomer and at 4 °C, however, the stability of the tetrameric structures were significantly low (T_m = 21.6–49.9 °C) (Fig. 2.7). Phe328 and Phe338 are located in the hydrophobic core and these amino acid residues stabilized the tetrameric structure through a π-interaction. Mutation of Phe328 to Val or Phe338 to Ile strongly destabilized the structure (T_m = 37.9 and 36.8 °C, respectively) even if Val and Ile were hydrophobic amino acids. This suggests that the aromaticity of Phe328 and Phe338 is important for the tetrameric structure. Mutation of Leu330,

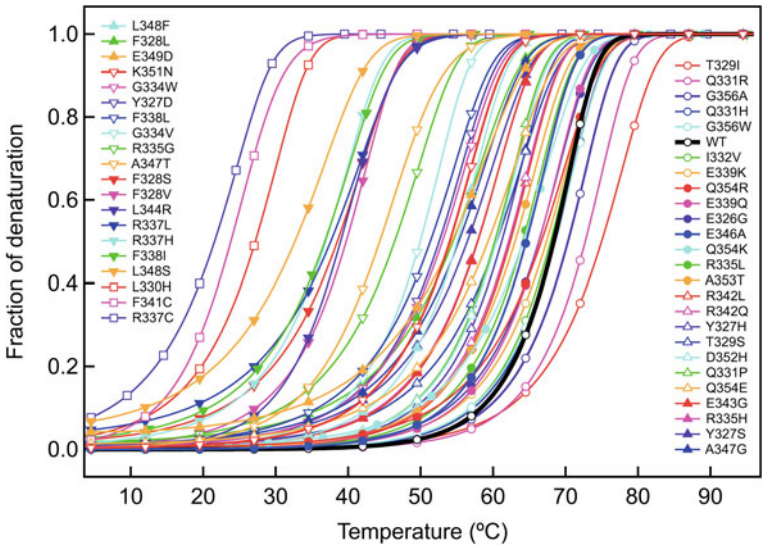

Fig. 2.5 Thermal denaturation of WT- and mutant-p53TD peptides. Thermal denaturation of the peptides was analyzed by measuring the ellipticity at 222 nm for peptide solutions containing 10 μM peptide in 50 mM sodium phosphate, pH 7.5, 100 mM NaCl over the range of 4–96 °C, with a scan rate of 1 °C/min

which is located in the center of the hydrophobic core, to Pro or Arg disrupted the tetramer and resulted in unfolded monomers. In contrast, L330H could form a tetrameric structure at low temperature. Under physiological pH, the His residues were not protonated because the basicity of the His residue was lower than the Arg residue. G334V and G334W induced a β-strand rich conformation and aggregation. Mutation of Gly334 to Val destabilized the turn and the G334V peptide formed an amyloid-like fibril under physiological conditions [32, 33]. Mutation of Arg335 to Gly, which resulted in the loss of the methylene group, strongly destabilized the tetrameric structure. There is a hydrophobic interaction between methylene group of Arg335 and the aromatic ring of Phe338. Mutations of Arg337 to His or Leu resulted in a strong destabilization (T_m = 36.9 and 37.6 °C, respectively) of the structure. Arg337 forms a salt-bridge with Asp352, and the methylene group of Arg337 likely interacts with nearby hydrophobic residues. Mutation of Arg337 to Leu was more destabilizing than mutation to His. The stability of R337H has been shown to be highly sensitive to pH within the physiological range [33]. Under the conditions used in the CD experiments, His had an overall positive charge like Arg. Therefore, R337H was slightly more stable than R337L. Mutation of the Leu348 residue which is buried at the tetramer interface, to Ala resulted in a dimer not a tetramer [18, 34]. This suggested that Leu348 stabilized the tetrameric structure through hydrophobic interactions. Mutation of Leu348 to Ser induced significant destabilization of the structure. In contrast, mutation to a hydrophobic amino acid residue Phe had little impact on the structure.

Table 2.3 Thermodynamic parameters for the mutant peptides

No.	mutant	State	T_m (°C)	ΔH_u^{Tm} (kcal/mol)	$\Delta\Delta G_u^{Tm}$ (kcal/mol)	K_d (nM)	WT AA
	WT	M-T	68.4 ± 0.3	166.0 ± 7.0	0.0	10.2	
1	E326G	M-T	66.3 ± 0.2	134.0 ± 3.8	0.8	63.5	solvent-exposed
2	Y327D	M-T	52.6 ± 0.1	111.8 ± 2.6	6.1	787.3	intermonomer with 331, 333
3	Y327H	M-T	61.2 ± 0.3	135.7 ± 6.3	3.0	113.1	intermonomer with 331, 333
4	Y327S	M-T	56.4 ± 0.1	102.6 ± 2.1	4.1	647.2	intermonomer with 331, 333
5	F328L	M-T	54.5 ± 0.3	94.1 ± 3.7	4.5	1020.0	π-interaction with Phe338, dimer core
6	F328S	M-T	39.9 ± 0.4	81.0 ± 4.9	9.5	6740.0	π-interaction with Phe338, dimer core
7	F328 V	M-T	39.7 ± 0.2	115.8 ± 4.8	12.8	5860.0	π-interaction with Phe338, dimer core
8	T329I	M-T	73.2 ± 0.2	126.4 ± 2.7	−1.7	48.0	solvent-exposed
9	T329S	M-T	60.5 ± 0.2	108.7 ± 2.3	2.7	347.2	solvent-exposed
10	L330H	M-T	27.2 ± 0.5	103.4 ± 7.4	18.8	72100.0	center of the hydrophobic core, dimer core
11	L330P	M					center of the hydrophobic core, dimer core
12	L330R	M					center of the hydrophobic core, dimer core
13	Q331H	M-T	68.6 ± 0.2	149.6 ± 6.8	−0.1	22.6	intermonomer with 327
14	Q331P	M-T	60.2 ± 0.2	133.9 ± 4.8	3.4	137.8	intermonomer with 327
15	Q331R	M-T	72.7 ± 0.3	156.9 ± 6.6	−1.9	9.0	intermonomer with 327
16	I332 V	M-T	67.9 ± 0.2	151.3 ± 4.3	0.2	22.6	buried in the hydrophobic core, dimer core
17	G334 V	M-T-A	49.9 ± 0.2	128.5 ± 4.1	8.2	787.7	a tight turn
18	G334 W	M-T	53.0 ± 0.2	110.2 ± 2.5	5.8	777.2	a tight turn
19	R335G	M-T	46.4 ± 0.7	100.5 ± 26.5	8.2	2290.0	solvent-exposed
20	R335H	M-T	57.8 ± 0.2	118.5 ± 3.5	4.1	327.2	solvent-exposed
21	R335L	M-T	64.1 ± 0.2	137.9 ± 3.0	1.8	70.0	solvent-exposed
22	R337C	M-T-A	21.6 ± 0.7	92.0 ± 21.7	20.6	196000.0	salt-bridge with Asp352, hydrophobic core
23	R337H	M-T	36.9 ± 0.2	104.0 ± 3.7	13.2	10200.0	salt-bridge with Asp352, hydrophobic core
24	R337L	M-T	37.6 ± 0.4	81.5 ± 4.6	10.6	9200.0	salt-bridge with Asp352, hydrophobic core
25	R337P	M					salt-bridge with Asp352, hydrophobic core

Table 2.3 (continued)

No.	mutant	State	T_m (°C)	ΔH_u^{Tm} (kcal/mol)	$\Delta\Delta G_u^{Tm}$ (kcal/mol)	K_d (nM)	WT AA
26	F338I	M-T	36.8 ± 0.5	93.0 ± 7.0	12.1	10400.0	π-interaction with Phe328, dimer core
27	F338L	M-T	51.3 ± 0.1	103.3 ± 3.6	6.2	1140.0	π-interaction with Phe328, dimer core
28	E339 K	M-T	67.4 ± 0.2	134.9 ± 2.7	0.4	53.9	solvent-exposed
29	E339Q	M-T	66.4 ± 0.2	141.1 ± 4.9	0.8	45.2	solvent-exposed
30	F341C	M-D	23.8 ± 0.3	66.4 ± 3.3	15.4	64400.0	hydrophobic core, tetramer interface
31	R342L	M-T	62.4 ± 0.2	137.3 ± 4.9	2.5	90.2	dimer core, solvent-exposed
32	R342P	M					dimer core, solvent-exposed
33	R342Q	M-T	62.1 ± 0.2	134.9 ± 4.1	2.6	102.4	dimer core, solvent-exposed
34	E343G	M-T	57.9 ± 0.2	120.7 ± 4.0	4.1	302.3	mc interdimer H-bond with sc351
35	L344P	M					hydrophobic core, tetramer interface
36	L344R	M-D	39.0 ± 0.2	71.4 ± 2.8	9.0	7900.0	hydrophobic core, tetramer interface
37	E346A	M-T	64.6 ± 0.1	145.1 ± 3.4	1.7	47.7	solvent-exposed
38	A347G	M-T	55.3 ± 0.2	100.1 ± 2.8	4.4	793.4	tetramer interface
39	A347T	M-D	44.3 ± 0.4	62.2 ± 4.7	6.2	4967.5	tetramer interface
40	L348F	M-T	55.0 ± 0.2	128.6 ± 4.8	5.7	347.3	hydrophobic core, tetramer interface
41	L348S	M-T	32.6 ± 0.3	76.4 ± 4.6	12.3	18500.0	hydrophobic core, tetramer interface
42	E349D	M-T	54.3 ± 0.2	82.6 ± 2.6	4.1	1450.0	sc intermonomer H-bond with mc333
43	K351 N	M-T	54.0 ± 0.4	117.9 ± 3.1	5.7	549.5	solvent-exposed
44	D352H	M-T	60.6 ± 0.2	133.0 ± 4.3	3.3	138.1	forms a salt-bridge with Arg337
45	A353T	M-T	63.0 ± 03	128.5 ± 4.8	2.1	119.3	solvent-exposed
46	Q354E	M-T	59.3 ± 0.3	99.8 ± 4.1	2.9	539.6	solvent-exposed
47	Q354 K	M-T	64.1 ± 0.2	113.9 ± 3.1	1.5	197.3	solvent-exposed
48	Q354R	M-T	66.7 ± 0.2	117.2 ± 10.0	0.6	134.9	solvent-exposed
49	G356A	M-T	70.3 ± 0.2	152.4 ± 4.7	−0.9	15.6	solvent-exposed
50	G356 W	M-T	68.5 ± 0.2	145.0 ± 4.7	−0.1	28.6	solvent-exposed

[a] The fraction of tetramer determined by gel filtration chromatography; asterisks indicate the fraction of dimer. M-T (Monomer–Tetramer); M-D (Monomer–Dimer); M (Monomer); T_m (transition temperature); ΔH^{Tm} (variation in the enthalpy of unfolding at T_m); $\Delta\Delta G_u^{Tm}$ (the difference in ΔG between WT and mutant peptides at the T_m of the WT peptide); sc (side chain); mc (main chain). The standard errors of fittings are indicated. The dissociation constant at 37 °C is calculated by $K_d = ((1-K_u)/2)^{-1/3}$. For dimer mutants, we used $K_d = K_u^{-1}$

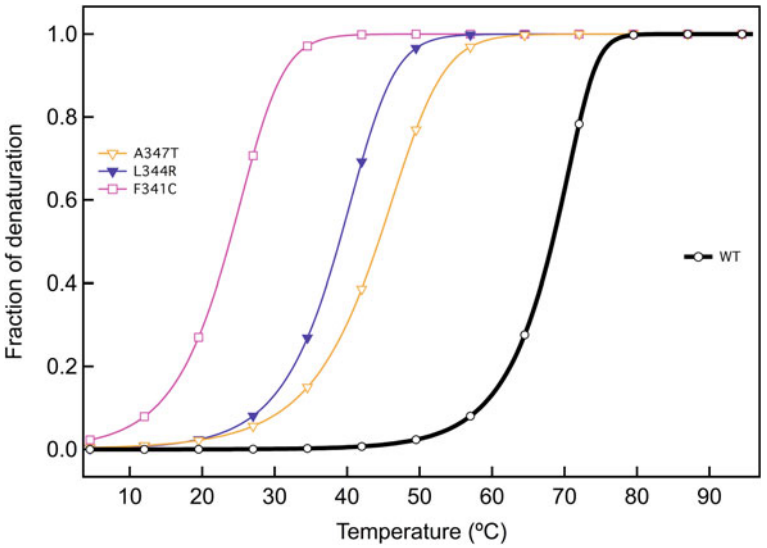

Fig. 2.6 Thermal denaturation of WT- and three dimer mutant-p53TD peptides (F341C, L344R, and A347T). Thermal denaturation of the peptides was analyzed by measuring the ellipticity at 222 nm for peptide solutions containing 10 μM peptide in 50 mM sodium phosphate, pH 7.5, 100 mM NaCl over the range of 4–96 °C, with a scan rate of 1 °C/min

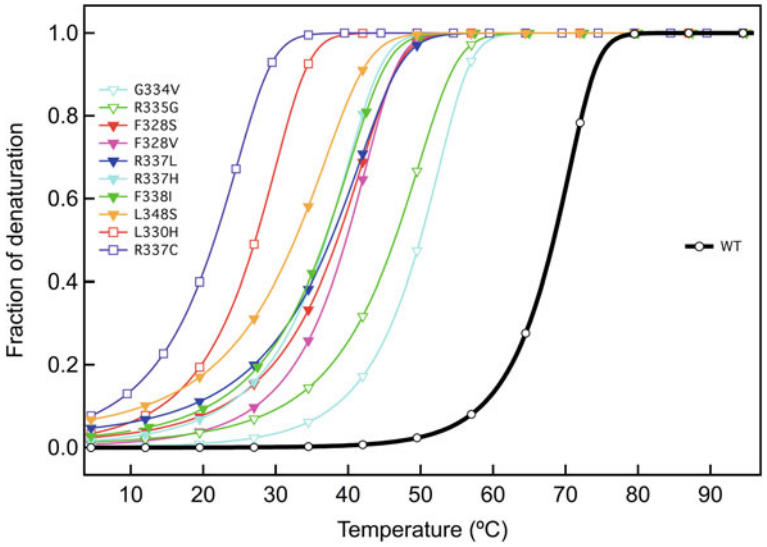

Fig. 2.7 Thermal denaturation of WT- and ten mutant-p53TD peptides (F328V, F328S, L330H, G334V, R335G, R337C, R337L, R337H, F338I, and L348S). Thermal denaturation of the peptides was analyzed by measuring the ellipticity at 222 nm for peptide solutions containing 10 μM peptide in 50 mM sodium phosphate, pH 7.5, 100 mM NaCl over the range of 4–96 °C, with a scan rate of 1 °C/min

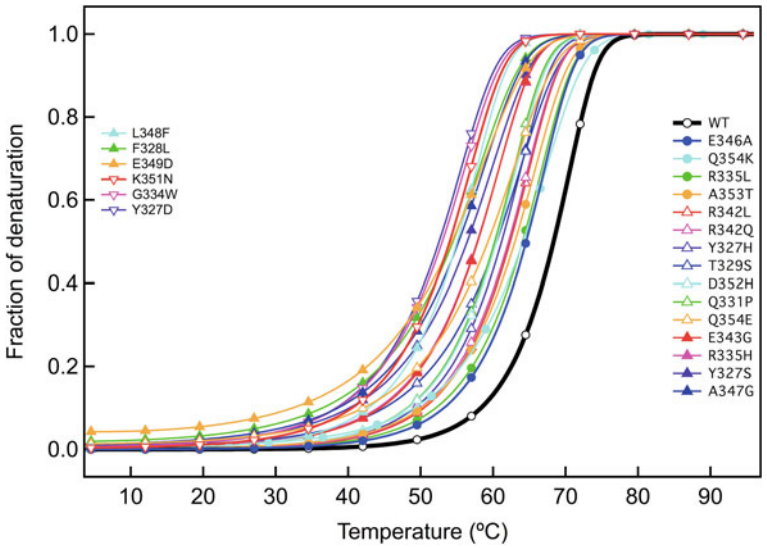

Fig. 2.8 Thermal denaturation of WT- and twenty-one mutant peptides (Y327D/H/S, F328L, T329S, Q331P, G334W, R335H/L, F338L, R342L/Q, E343G, E346A, A347G, L348F, E349D, K351 N, D352H, A353T, Q354E, and Q354K). Thermal denaturation of the peptides was analyzed by measuring the ellipticity at 222 nm for peptide solutions containing 10 μM peptide in 50 mM sodium phosphate, pH 7.5, 100 mM NaCl over the range of 4–96 °C, with a scan rate of 1 °C/min

Twenty-two mutant peptides (Y327D/H/S, F328L, T329S, Q331P, G334W, R335H/L, F338L, R342L/Q, E343G, E346A, A347G, L348F, E349D, K351N, D352H, A353T, Q354E, and Q354K) were slightly or moderately destabilized (T_m = 51.3–64.6 °C) (Fig. 2.8). Mutation of Tyr327 to Asp, His, and Ser moderately destabilized the structure (T_m = 52.6, 61.2, and 56.4 °C, respectively). The aromatic ring of Tyr327 might interact with methylene group of Arg333. Y327H was more stable than Y327D and Y327S because His with an imidazole group is more hydrophobic than Asp or Ser. Mutation of Thr329 to Ser slightly destabilized the tetrameric structure. Effect of the mutation on the structure was expected to be small because the side chain of Thr329 was exposed to solvent. Interestingly, the Q331P peptide could form tetramers and the mutation had only small effects on the stability of the structure even though the Pro mutation is in the β-strand. R342L and R342Q were only slightly destabilized because the side chain of Arg342 is exposed to solvent. The mutant E349D was slightly destabilized (T_m = 54.3 °C). The effect of removal of a methylene group by mutation to Asp was small because the Glu349 residue is exposed to solvent. Asp352 forms a salt-bridge with Arg337. Mutation of Asp352 to His moderately destabilized the structure, although mutation of Arg337 was strongly destabilizing. These results suggested that an electrostatic interaction such as a salt-bridge was less crucial to the structure than a hydrophobic interaction. A353T, Q354E, and Q354K slightly destabilized the tetrameric structure, because Ala353 and Gln354 are exposed to solvent.

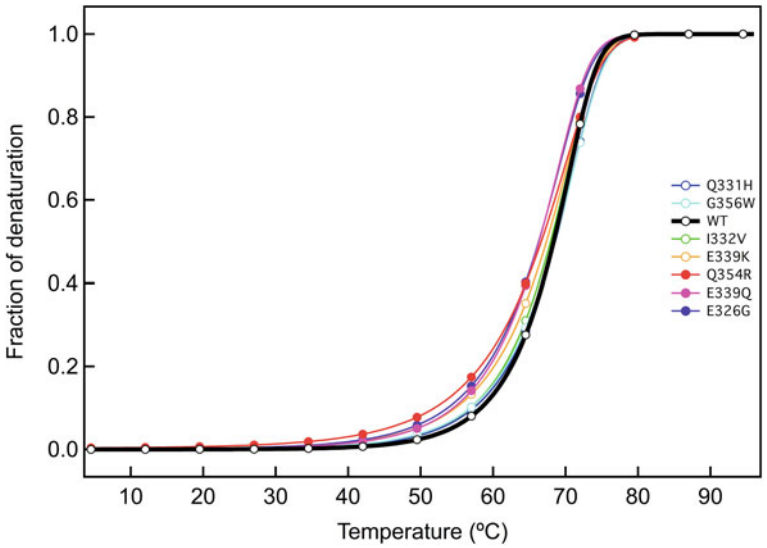

Fig. 2.9 Thermal denaturation of WT- and seven mutants (E326G, I332V, Q331H, E339K/Q, Q354R, and G356W). Thermal denaturation of the peptides was analyzed by measuring the ellipticity at 222 nm for peptide solutions containing 10 μM peptide in 50 mM sodium phosphate, pH 7.5, 100 mM NaCl over the range of 4–96 °C, with a scan rate of 1 °C/min

Seven mutants (E326G, I332V, Q331H, E339K/Q, Q354R, and G356W) showed almost the same stability as the WT (Fig. 2.9). Glu326 is located at the amino edge of a β-strand and exposed to the solvent. Mutation of Glu326 to Gly had little effect on the structure, although Gly has no side chain and does not tend to form a β-strand. I332V induced a limited change in the thermal stability of the tetrameric structures ($\Delta T_m = -0.5$ °C, $\Delta\Delta G_u^{Tm} = -0.2$ kcal/mol), even though Ile332 is buried at the hydrophobic core of the tetramer. Interestingly, the destabilization observed ($\Delta G_u^{Tm} = -0.2$ kcal/mol) was smaller than the average found for the removal of a buried methylene group in monomeric proteins. E339K, E339Q, and G356W showed almost same stability as WT. Glu339 and Gly356 are exposed to solvent and thus, their mutations did not affect the stability of the tetramer.

Three mutants (T329I, Q331R, and G356A) were more stable than WT ($T_m = 73.2$, 72.7, and 70.3 °C, respectively) (Fig. 2.10). Mutation of Glu331 to His or Arg slightly stabilized the tetrameric structure. It was expected that mutation of Gln331 would have little effect on the structure because the side chain of Gln331 is exposed to solvent. Intriguingly, Arg substitution for Gln331 caused an increase in stability of $\approx$4.3 °C. There are two possible reasons why Q331R stabilized the structure. One, the methylene group of Arg can stabilize the structure through hydrophobic interactions with amino acid residues around Gln331, such as the aromatic ring of Tyr327. Two, the cationic group of Arg can interact with the aromatic ring of Tyr327 by cation-π interaction. Gly356 is located at the carboxyl edge of an α-helix. Mutation of Gly356 to Ala results in a tendency to form an α-helix, which could in turn stabilize the tetrameric structure.

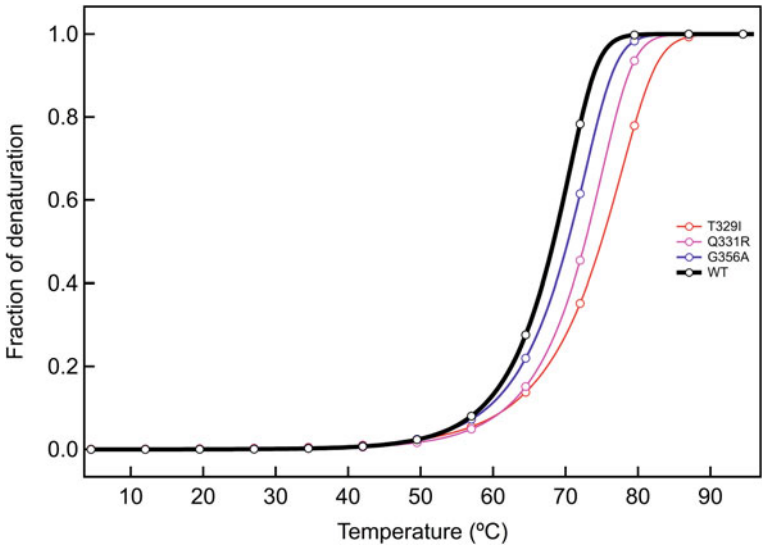

Fig. 2.10 Thermal denaturation of WT- and three mutants (T329I, Q331R, and G356A). Thermal denaturation of the peptides was analyzed by measuring the ellipticity at 222 nm for peptide solutions containing 10 μM peptide in 50 mM sodium phosphate, pH 7.5, 100 mM NaCl over the range of 4–96 °C, with a scan rate of 1 °C/min

2.3.5 Modeling of Mutant p53TD Peptides

Mutations that changed some solvent-exposed p53TD amino acid residues had little or no significant affect on the tetramers' thermal stability. To elucidate why these mutations occur in human cancers, the TD of each mutant were modeled (Fig. 2.12), finding that changes in some solvent-exposed residues altered the calculated electrostatic potential on the surface of the p53TD. This was especially so for E339K, E339Q, E343G, E346A, and Q354K. I suggest that these changes might influence either the interdomain or the intermolecular interactions with binding partners that thereby could account for their selection as cancer mutants.

2.3.6 Correlation Between Stability of p53TD Peptides and that of the Full-Length p53 Protein and the Transcriptional Activity

The stabilities of the tetrameric structures of the mutant p53TD peptides were compared with the oligomeric state of full-length p53-EGFP fusion proteins carrying TD mutations; FIDA was employed that yields a quantitative assessment of the fraction of protein oligomers in vivo at physiologically relevant concentrations

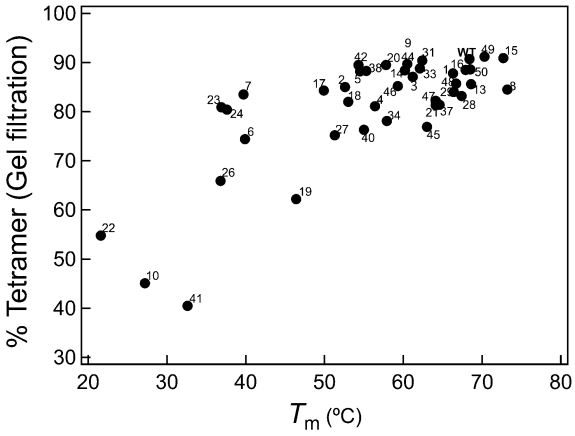

Fig. 2.11 Comparison of thermodynamic stability by CD and oligomeric status by gel filtration analysis. The T_m values of mutant peptides and the fraction of oligomers were obtained as shown in Table 2.2 and Table 2.3. The data for mutants are plotted as solid circles. Numbers refer to mutants as listed in Table 2.2. Monomer mutants 11, 12, 25, 32, and 35, and dimer mutants 30, 36, and 39 are not shown

[28]. The clear correlation ($r = 0.77$) between the T_m measured here and the in vivo oligomerization state (Fig. 2.13) strongly suggests that the quantitative data on the tetrameric structure of p53 peptides is extendable to the full p53 protein.

Also, the stabilities of the tetrameric structures were compared with the transcriptional activity of full-length EGFP-p53 protein with TD mutations, which were analyzed by p53 reporter system in living cell [28]. There were strong correlation between the T_m and the in vivo transcriptional activity (Fig. 2.14).

2.4 Discussion

In this study, I represent the first comprehensive, quantitative biophysical analysis of the oligomeric state and thermal stability of the 50 TD mutants identified in human cancers. Most mutant p53TD peptides formed a WT-like tetrameric structure with diminished stability (Fig. 2.4). However, tetrameric mutants with altered hydrophobic core residues (F328, L330, R337, F338, F341, L344, and L348), except I322V, exhibited dramatic reductions in stability and, in some cases, unfolding of the peptide (e.g. L330H, P, R; R337C, P; R342P, L344P) as determined by CD measurements (Fig. 2.3). In particular, mutations that introduced proline in the α-helix devastated tetramer formation; some mutants could not form tetramers and existed as unfolded monomers (L330P/R, R337P, R342P, and L344P), or as folded dimers (F341C, L344R, and A347T). Indeed, the thermal denaturation study predicted that several TD mutants (e.g. L330H, R337C/H/L, F338I, F341C, L344R, and L348S) are thermally unstable at or near body temperature. These results are consistent with an alanine-scanning study of the p53TD that identified nine key hydrophobic resides important for TD thermal stability and oligomerization [18].

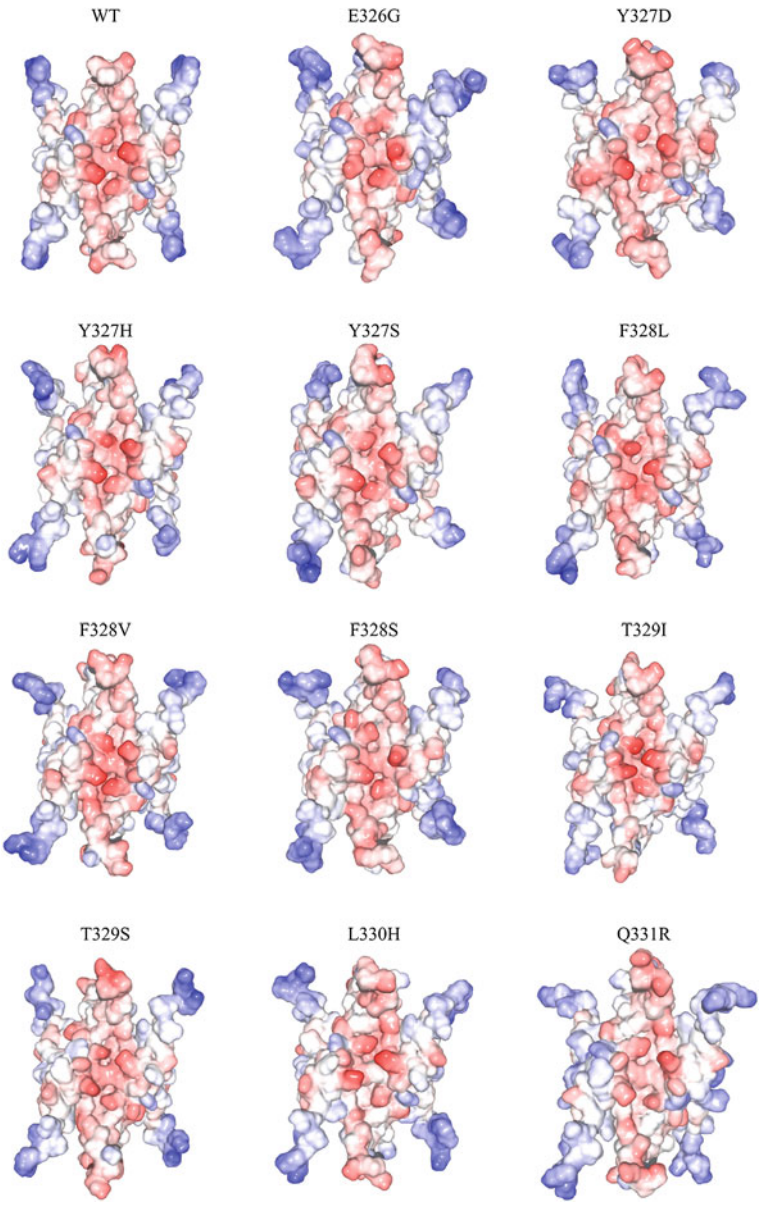

Fig. 2.12 The surface modeling of *mutant p53TDs.* A solvent exposed surface of the p53TD mutants, colored by electrostatic potential. The positively charged surface in *blue* and negative in *red*

In contrast to mutations that affect hydrophobic core residues, mutations that affect residues accessible to solvent were less destabilizing. The WT p53TD is thermally quite stable ($T_m \sim 70$ °C, Table 2.3) compared with the core DNA-binding domain

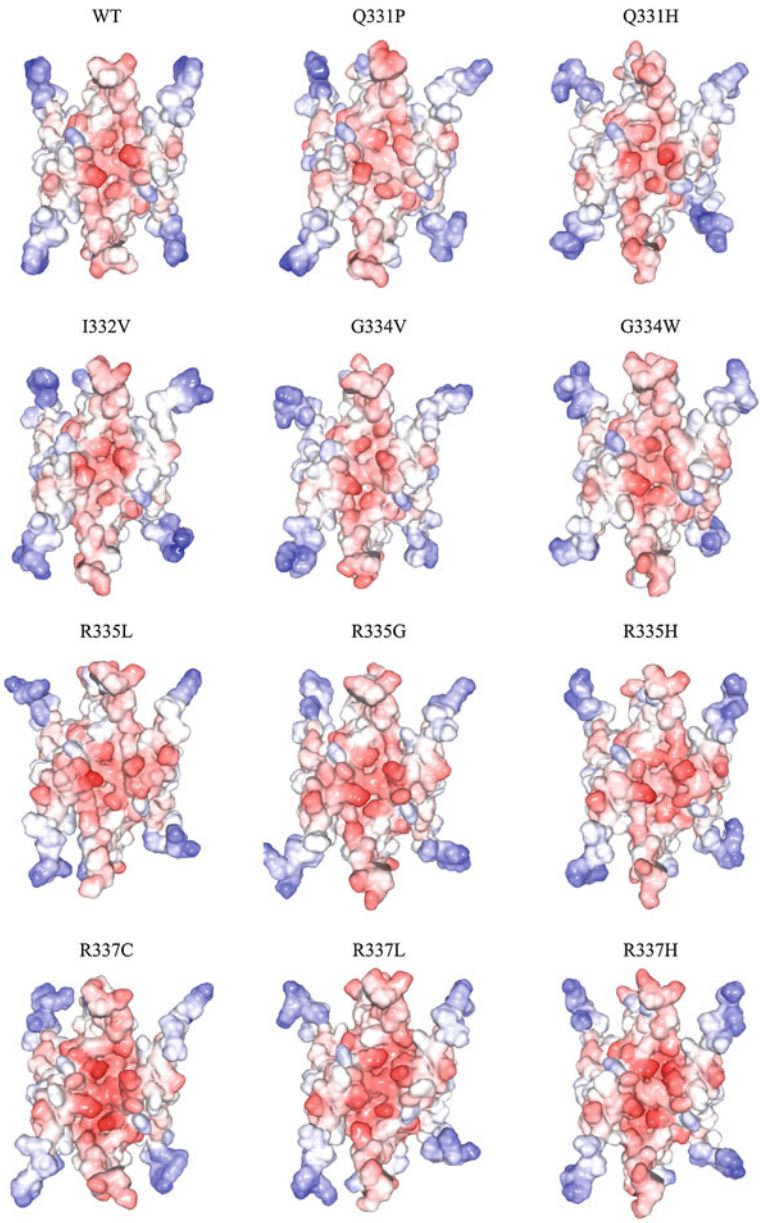

Fig. 2.12 continued

[15]; most mutations that affect TD domain residues, except as noted above, would not be expected to unfold the domain structure. Nevertheless, for most thermally stable TDs, the change in amino acids significantly altered the disassociation constant for tetramer formation (Table 2.3). Importantly, because tetramers are essential for DNA

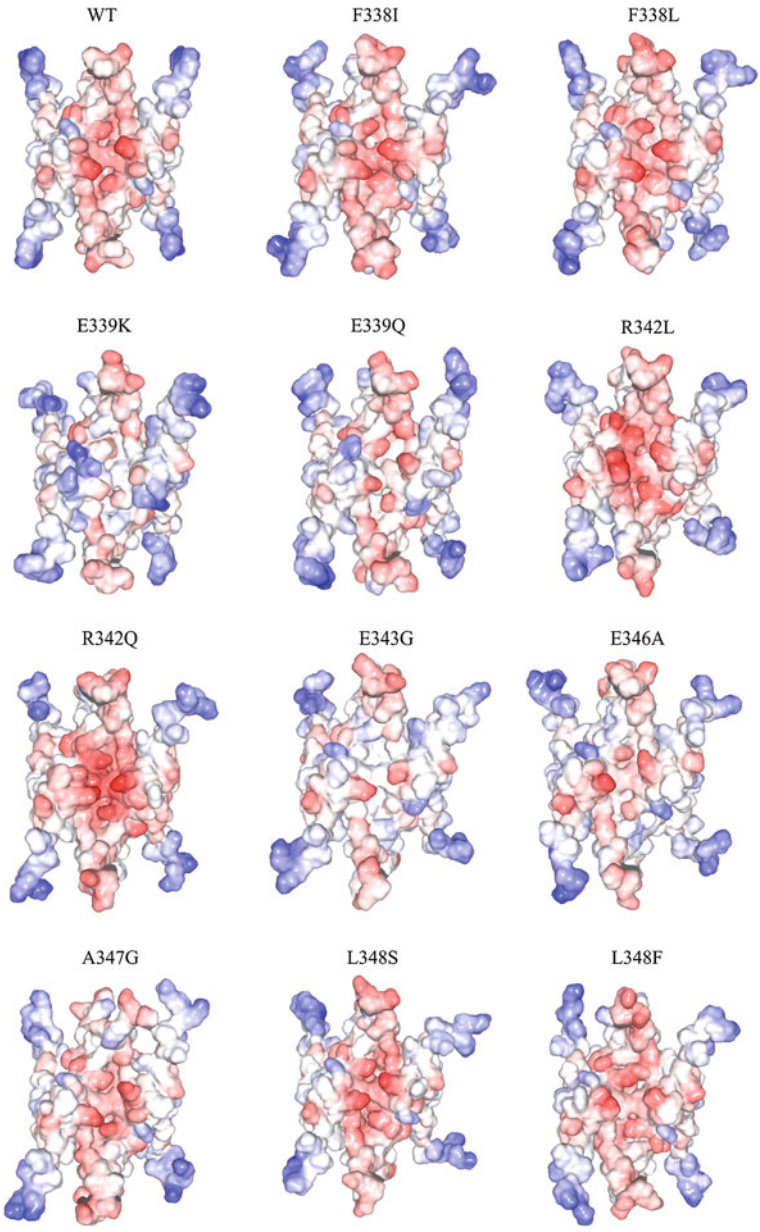

Fig. 2.12 continued

binding and activating transcription [9], and the p53 tetramer is in equilibrium with the monomer, the intra-nuclear p53 concentration is a critical factor in determining p53 function. In cultured, undamaged human embryonic skin fibroblasts (WS-1 cells), p53

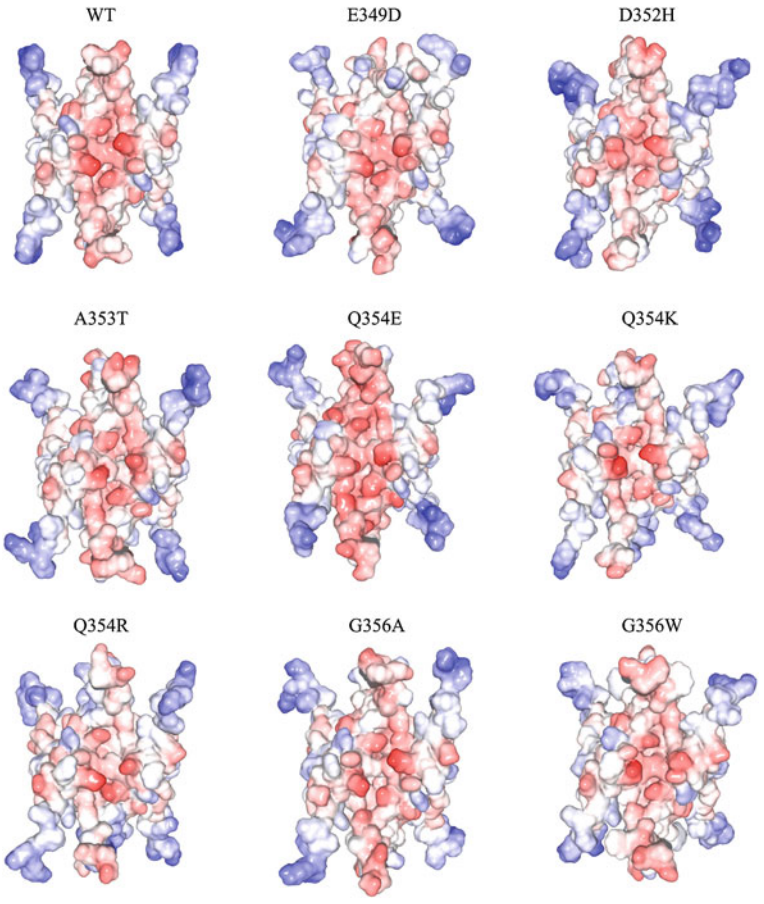

Fig. 2.12 continued

abundance was 7.8×10^3 molecules/cell, whereas after DNA damage from neocarzinostatin, it rose $\sim$ threefold to 21.8×10^3 molecules/cell [35]. The volume of the nucleus of a human fibroblast is about 10^{-12} L [36]. Correspondingly, the p53 concentration in the nucleus of normal, unstressed human cells is ≈ 13 nM and increases to ≈ 36 nM after DNA damage. At these concentrations, the fraction of tetramer for TD mutants at 37 °C can be assessed (Fig. 2.15). Thus, I predict that about 80 % of the accumulated WT p53 protein (WT p53TD $K_d = 10.2$ nM) is in the tetrameric state following DNA damage. These values might be somewhat high as the skin fibroblasts were cultured under normoxic conditions (~ 21 % oxygen), i.e., much higher that the oxygen concentration in most tissues (~ 5–8 %). Oxidative stress activates p53, and normoxia causes oxidative stress in cultured cells [32]. Nevertheless, the dissociation constant for the formation of the WT p53 tetramer seems tuned to accommodate a much greater change in p53 function than the $\sim$ threefold change in nuclear

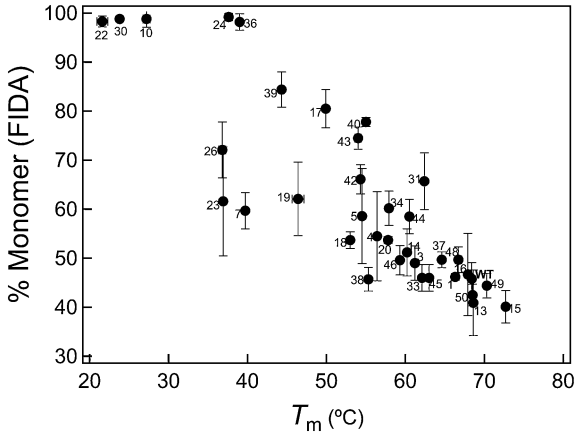

Fig. 2.13 Correlation between the T_m and the fraction of monomers of WT and mutant p53 protein estimated by FIDA. FIDA data for the fraction of monomer of p53 protein as reported by Imagawa et al. [28]. Fraction of monomers is plotted as a function of the stability of p53TD mutants obtained from the thermal denaturation data (Table 2.3)

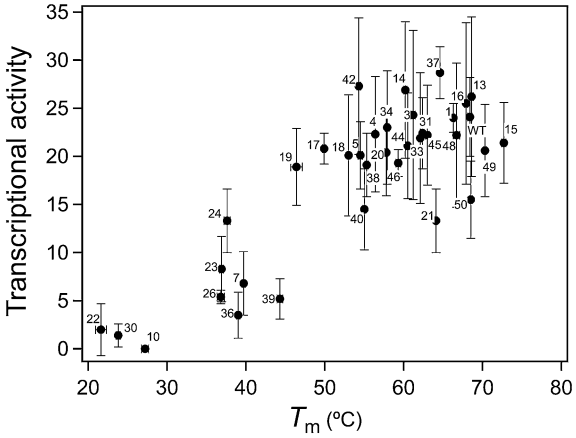

Fig. 2.14 Correlation between the T_m and the transcriptional activity of the mutant p53 protein estimated by reporter assay. The data for the transcriptional activity of p53 protein as reported by Imagawa et al. [28]. Transcriptional activity is plotted as a function of the stability of p53TD mutants obtained from the thermal denaturation data (Table 2.3)

concentration. Hence, cancer mutations that affect the p53TD K_d by more than $\sim$ 10-fold might not elicit a sufficient concentration of tetramers in cells to induce the transcriptional responses important for tumor suppression [3]. Additionally, p53-mediated transcription-independent apoptosis, which reportedly depends on the ability of p53 to form tetramers in the cytoplasm [12], might be diminished. Nevertheless, I argue that even mild changes to the K_d for tetramer formation or in p53 stability could significantly affect p53 function because of the sensitivity of tetramer formation to the K_d and p53 concentration in the physiological range. Many previous studies involved a $\sim$ 20-fold p53 overexpression (Fig. 2.16) that would not reveal the detrimental effects of many p53TD mutations (Fig. 2.17). These results suggested that care should be taken when p53 function is analyzed under nonnative conditions, such as in a transient expression system, where the protein concentration is very high.

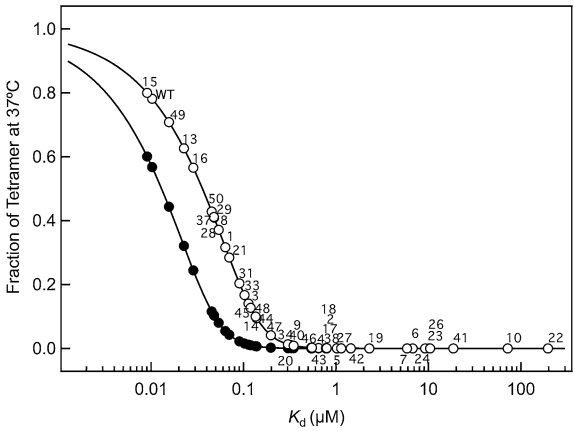

Fig. 2.15 Fraction of tetramer at 37 °C at concentrations of 13 nM (endogenous p53 level in unstressed cell) and 36 nM (stressed cell) against the value of K_d. Each data point represents the value of a mutant at 13 nM (solid circles) and 36 nM (open circles). Monomer mutants 11, 12, 25, 32, and 35, and dimer mutants 30, 36, and 39 are not shown

In addition to the direct effects of mutations on tetramer formation, several indirect effects may further acerbate p53 function (Fig. 2.18). First, the p53TD contains a nuclear export signal (NES, M340-K351) that is exposed in the monomer and dimer but not in the tetramer [33]. Except for those mutants in the α-helix between M340 and K351 that affect the interaction of the NES with CRM1 [33], TD mutants potentially could acerbate tetramer formation by increasing the cytoplasmic export of p53 and preventing its nuclear accumulation to normal levels. Second, several post-translational modifications that potentially modulate p53 activity are influenced by its oligomeric state, and the oligomeric state can be modulated by post-translational modifications. The phosphorylation of Ser392 enhances tetramer formation [30]. The p53TD peptide in which His replaced L330 was thermally destabilized (Table 2.3), and the phosphorylation of p53 Ser392 by casein kinase 2 was diminished when L330 was mutated to His [37]. Deletion of the residues 334–354 abolishes the ability of Chk1 to phosphorylate p53 [8]; sites that Chk1 can phosphorylate are believed to modulate p53 activity and stability [4]. The PCAF acetyltransferase, which acetylates Lys320, specifically recognizes p53′s tetrameric structure [6]. In addition, Pirh2, an E3 ubiquitin protein-ligase that binds and ubiquitylates p53 protein in vitro and in vivo, only acts on its tetrameric form [38].

More than 50 proteins reportedly interact with the C-terminal region of the p53 protein, and several of them either require or influence tetramer formation. Tetramer formation of p53 is essential for its interaction with HPV-16 E2, c-Abl, and Mdm2 [9, 21]. The binding affinity of p53 to MDM2 fell when p53 contained the mutation L344P or R337C found in Li-Fraumeni patients [21]. c-Abl binds directly to the C-terminal basic domain of p53, and this interaction requires a tetramer. c-Abl may stabilize the tetrameric conformation, resulting in a more stable p53-DNA complex [39]. In contrast, the interaction of ARC with the p53TD inhibits tetramer formation and increases nuclear export [40]. The binding of S100 family proteins depends on the oligomeric status of p53 and controls the balance between monomer and tetramer [41]. Binding of the 14-3-3 protein to p53 enhances sequence-specific DNA binding by inducing p53 to form tetramers at lower concentrations [42].

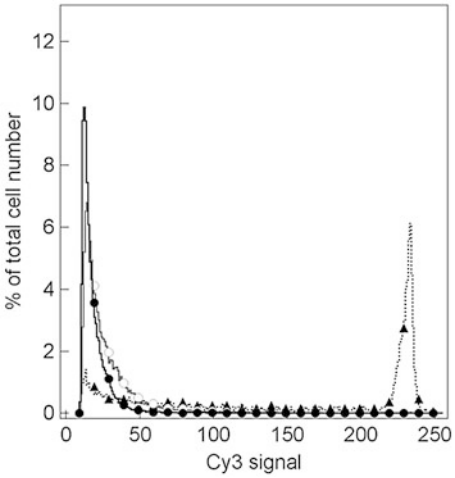

Fig. 2.16 Fraction of tetramer at 37 °C in cells when overexpressed. H1299 cells (p53 null) were transiently transfected p53 expression vector. The H1299 cells and A549 cells (expressed wild-type p53) with or without UV (25 J/m^2) treatment were stained with anti-p53 monoclonal antibody (DO-1) and Cy3-conjugated secondary antibody. The Cy3 signal intensity of each cell was measured and the distributions of Cy3 signal intensity are shown; A549 (endogenous p53 level without UV; *solid circle*, *solid line*), A549 (endogenous p53 level with UV; *open circle*, *solid gray line*), and H1299 (transient transfection; *solid triangle*, *dotted line*). The detailed methods were described as previously [28]

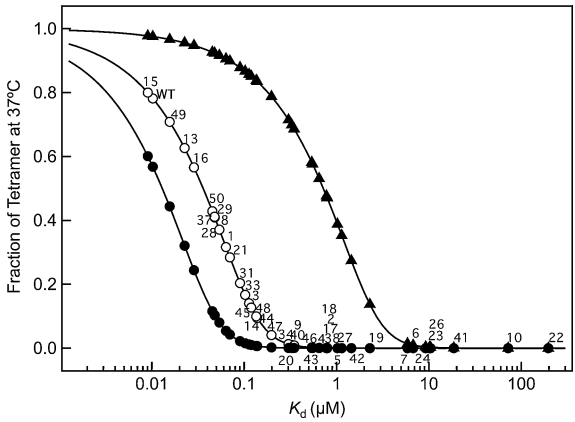

Fig. 2.17 Fraction of tetramer at 37 °C in cells when overexpressed. **b** Each data point represents the value of a mutant at 36 nM, endogenous p53 level in stressed cell, (open circles) and 720 nM, p53 level in cell when overexpressed, (*solid triangles*). Monomer mutants 11, 12, 25, 32, and 35, and dimer mutants 30, 36, and 39 are not shown

The p53TD from ∼ 13 apparently cancer-associated mutants in eight residues, mostly in the α-helical region of the TD, only moderately affected, by ∼fivefold, the K_d of tetramer formation of E326G, T329I, R335L, E339 K, E339Q, and E346A, and very slightly affected, by twofold, that of Q331H, Q331R, I332 V, G356A and G356 W (Table 2.3). The apparently minimal effect of these changes

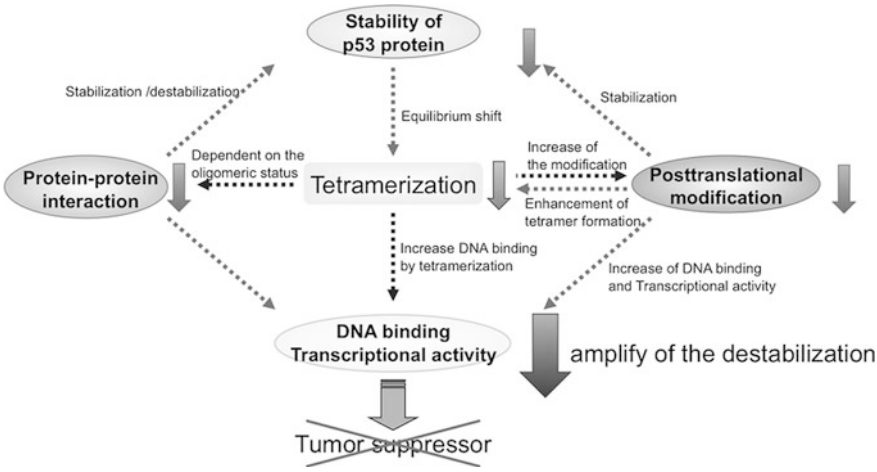

Fig. 2.18 Amplification of the destabilization effects of mutations. Tumor suppressor activity of p53 is regulated by many factors, including tetramerization, posttranslational modification, protein–protein interactions. Mutations of tetramerization domain directly destabilize the tetrameric structure and decrease p53 function (*dark gray arrow*). Because tetramer formation is crucial for posttranslational modification, DNA binding, and protein–protein interactions, destabilization of the tetrameric structure decreases them. Thus, mutations of tetramerization domain indirectly affect the posttranslational modification and protein–protein interactions and result in more destabilization of the structure and decrease function

is particularly surprising for mutations that affect E326, I332, E339, and E346, because these are among the 12 most highly evolutionarily conserved residues in the TD [9], and changes to conserved residues often are deleterious to function. I questioned why then do the mutations causing these changes exist among p53-associated cancer mutants? As Soussi et al. noted [43], mistakes occur in the literature on p53, possibly due to errors in sequencing or PCR, so caution is needed about accepting mutants that have been reported in cancers only once or a few times; data on germline mutants should be more reliable. Of the 13 mutants noted above, all but four (Q331H, Q331R, R342Q, G356W) occur only once in the IARC TP53 mutant database (http://www-p53.iarc.fr/), and none have been reported as germline mutations. Thus, some of these mutants may be false reportings. Of the remaining four mutants (Fig. 2.12), two clearly are solvent exposed residues that either change the surface charge (R342Q) or replace a small residue with one bearing a bulky, hydrophobic side chain at the surface (G356W). Although mutations affecting solvent exposed residues and altering the electrostatic potential of p53′s surface were less thermally destabilizing than core mutants were, the change in surface charge potential might well affect intra-protein interactions or the interaction of the TD with one or more of its many binding partners. R342Q represents such a change, and the G356W change might disrupt surface complementarity that could affect protein interactions important for p53′s function. Many mutants with greatly changed K_ds also involve surface-exposed alterations in

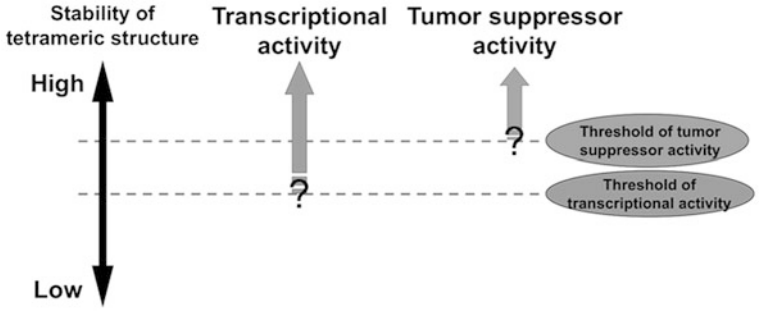

Fig. 2.19 Threshold for loss of tumor suppressor activity of p53 in terms of the disruption of tetrameric structure. The stability of tetrameric structure is correlated with the transcriptional activity of p53. From our results, it was suggested that the threshold for loss of tumor suppressor activity in terms of the disruption of p53′s tetrameric structure could be extremely low

charge that affect the predicted electrostatic potential of the p53TD′s surface (Fig. 2.3). In the crystal structure, E349D, a change that moderately increases the K_d (to 1450 nM) is implicated in crystal contacts and, therefore, probably is important for such interactions [44].

Residue Q331 is in the short β-sheet that forms part of the monomer–monomer interface, but Q331 is not involved in monomer–monomer interactions, and the change to either His, Arg, or even Pro had only minor effects on p53TD thermal stability (Table 2.3). A recent yeast-based assay for transcriptional activation revealed that almost any amino acid sufficed at this position [45]. Thus, biophysical or biochemical measurements do not show why mutations that alter this residue appear among cancer-associated ones.

Analyses of SNPs in p53 and its pathway support the suggestion of the potential importance of the subtle effects of TD mutants on tetramer formation. The *TP53* gene reportedly contains nineteen exonic polymorphisms, among which researchers have validated four (R47S, R72P, V217M, and G360A). The codon 47P/S and 72R/P polymorphisms subtly alter expression of p53 transcriptional targets. Although controversial [46], molecular evidence suggests that both polymorphisms alter cancer risk [47–49]. Additional evidence comes from SNPs in p53 pathways. Bond et al., working on the most intensively studied T/G SNP at nucleotide 309 in the first intron of the *MDM2* gene, demonstrated that the 309G variant is bound more efficiently by the transcription factor SP1, thereby increasing the efficiency of synthesizing MDM2, and consequently, slightly lowering levels of p53 [50]. The estrogen receptor also binds the *MDM2* promoter in the region of SNP309 and also can increase MDM2 expression in response to the hormone. Several studies associated MDM2 SNP309 polymorphism and increased cancer risk in males and females, although others saw no such connection [46]. Thus, although further work is required, these studies support the hypothesis that relatively small changes in p53 concentration or the ability to form tetramers could contribute to cancer risk or progression. I suggest that the threshold for loss of

tumor suppressor activity in terms of the disruption of p53′s tetrameric structure could be extremely low (Fig. 2.19). Furthermore, the study of cancer-associated mutants in the TD that minimally affect tetramer formation may reveal additional functions for this domain in p53 biology. The main result in this chapter was published first in *Journal of Biological Chemistry* in 2011, and this chapter is its expanded version [51].

References

1. Hanahan D, Weinberg RA (2000) The hallmarks of cancer. Cell 100:57–70
2. Halazonetis TD, Gorgoulis VG, Bartek J (2008) An oncogene-induced DNA damage model for cancer development. Science 319:1352–1355
3. Zilfou JT, Lowe SW (2009) Tumor suppressive functions of p53. Cold Spring Harb Perspect Biol 2:a000935–a000935
4. Meek DW, Anderson CW (2009) Posttranslational modification of p53: cooperative integrators of function. Cold Spring Harb 1–16: 528–536
5. Halazonetis TD, Kandil AN (1993) Conformational shifts propagate from the oligomerization domain of p53 to its tetrameric DNA binding domain and restore DNA binding to select p53 mutants. EMBO J 12:5057–5064
6. Sakaguchi K, Herrera JE, Saito S, Miki T, Bustin M, Vassilev A, Anderson CW, Appella E (1998) DNA damage activates p53 through a phosphorylation-acetylation cascade. Genes Dev 12:2831–2841
7. Maki CG (1999) Oligomerization is required for p53 to be efficiently ubiquitinated by MDM2. J Biol Chem 274:16531–16535
8. Shieh SY, Ahn J, Tamai K, Taya Y, Prives C (2000) The human homologs of checkpoint kinases Chk1 and Cds1 (Chk2) phosphorylate p53 at multiple DNA damage-inducible sites. Genes Dev 14:289–300
9. Chene P (2001) The role of tetramerization in p53 function. Oncogene 20:2611–2617
10. Warnock LJ, Knox A, Mee TR, Raines SA, Milner J (2008) Influence of tetramerisation on site-specific post-translational modifications of p53: comparison of human and murine p53 tumor suppressor protein. Cancer Biol Ther 7:1481–1489
11. Itahana Y, Ke H, Zhang Y (2009) p53 Oligomerization is essential for its C-terminal lysine acetylation. J Biol Chem 284:5158–5164
12. Pietsch EC, Perchiniak E, Canutescu AA, Wang G, Dunbrack RL, Murphy ME (2008) Oligomerization of BAK by p53 utilizes conserved residues of the p53 DNA binding domain. J Biol Chem 283:21294–21304
13. Hainaut P, Hollstein M (2000) p53 and human cancer: the first ten thousand mutations. Adv Cancer Res 77:81–137
14. Petitjean A, Mathe E, Kato S, Ishioka C, Tavtigian SV, Hainaut P, Olivier M (2007) Impact of mutant p53 functional properties on TP53 mutation patterns and tumor phenotype: lessons from recent developments in the IARC TP53 database. Hum Mutat 28:622–629
15. Joerger AC, Fersht AR (2010) The tumor suppressor p53: from structures to drug discovery. Cold Spring Harb Perspect 2(6):a000919–a000919
16. Clore GM, Ernst J, Clubb R, Omichinski JG, Kennedy WMP, Sakaguchi K, Appella E, Gronenborn AM (1995) Refined solution structure of the oligomerization domain of the tumour suppressor p53. Nat Struct Biol 2:321–333
17. Jeffrey PD, Gorina S, Pavletich NP (1995) Crystal structure of the tetramerization domain of the p53 tumor suppressor at 1.7 angstroms. Science 267:1498–1502

18. Mateu MG, Fersht AR (1998) Nine hydrophobic side chains are key determinants of the thermodynamic stability and oligomerization status of tumour suppressor p53 tetramerization domain. EMBO J 17:2748–2758
19. DiGiammarino EL, Lee AS, Cadwell C, Zhang W, Bothner B, Ribeiro RC, Zambetti G, Kriwacki RW (2002) A novel mechanism of tumorigenesis involving pH-dependent destabilization of a mutant p53 tetramer. Nat Struct Biol 9:12–16
20. Davison TS, Yin P, Nie E, Kay C, Arrowsmith CH (1998) Characterization of the oligomerization defects of two p53 mutants found in families with Li-Fraumeni and Li-Fraumeni-like syndrome. Oncogene 17:651–656
21. Lomax ME, Barnes DM, Hupp TR, Picksley SM, Camplejohn RS (1998) Characterization of p53 oligomerization domain mutations isolated from Li-Fraumeni and Li-Fraumeni like family members. Oncogene 17:643–649
22. Atz J, Wagner P, Roemer K (2000) Function, oligomerization, and conformation of tumor-associated p53 proteins with mutated C-terminus. J Cell Biochem 76:572–584
23. Rollenhagen C, Chene P (1998) Characterization of *p53* mutants identified in human tumors with a missense mutation in the tetramerization domain. Int J Cancer 78:372–376
24. Johnson CR, Morin PE, Arrowsmith CH, Freire E (1995) Thermodynamic analysis of the structural stability of the tetrameric oligomerization domain of p53 tumor suppressor. Biochemistry 34:5309–5316
25. Maki CG, Huibregtse JM, Howley PM (1996) In vivo ubiquitination and proteasome-mediated degradation of p53(1), Cancer Res 56:2649–2654
26. Kato S, Han SY, Liu W, Otsuka K, Shibata H, Kanamaru R, Ishioka C (2003) Understanding the function-structure and function-mutation relationships of p53 tumor suppressor protein by high-resolution missense mutation analysis. Proc Natl Acad Sci USA 100:8424–8429
27. Kawaguchi T, Kato S, Otsuka K, Watanabe G, Kumabe T, Tominaga T, Yoshimoto T, Ishioka C (2005) The relationship among p53 oligomer formation, structure and transcriptional activity using a comprehensive missense mutation library. Oncogene 24:6976–6981
28. Imagawa T, Terai T, Yamada Y, Kamada R, Sakaguchi K (2009) Evaluation of transcriptional activity of p53 in individual living mammalian cells. Anal Biochem 387:249–256
29. Nomura T, Kamada R, Ito I, Chuman Y, Shimohigashi Y, Sakaguchi K (2009) Oxidation of methionine residue at hydrophobic core destabilizes p53 tetrameric structure. Biopolymers 91:78–84
30. Sakaguchi K, Sakamoto H, Lewis MS, Anderson CW, Erickson JW, Appella E, Xie D (1997) Phosphorylation of serine 392 stabilizes the tetramer formation of tumor suppressor protein p53. Biochemistry 36:10117–10124
31. Šli A, Blundell TL (1993) Comparative protein modelling by satisfaction of spatial restraints. J Mol Biol 234:779–815
32. Parrinello S, Samper E, Krtolica A, Goldstein J, Melov S, Campisi J (2003) Oxygen sensitivity severely limits the replicative lifespan of murine fibroblasts. Nat Cell Biol 5:741–747
33. Stommel JM, Marchenko ND, Jimenez GS, Moll UM, Hope TJ, Wahl GM (1999) A leucine-rich nuclear export signal in the p53 tetramerization domain: regulation of subcellular localization and p53 activity by NES masking. EMBO J 18:1660–1672
34. Fernandez-Fernandez MR, Veprintsev DB, Fersht AR (2005) Proteins of the S100 family regulate the oligomerization of p53 tumor suppressor. Proc Natl Acad Sci USA 102:4735–4740
35. Wang YV, Wade M, Wong E, Li YC, Rodewald LW, Wahl GM (2007) Quantitative analyses reveal the importance of regulated Hdmx degradation for p53 activation. Proc Natl Acad Sci USA 104:12365–12370
36. Swanson JA, Lee M, Knapp PE (1991) Cellular dimensions affecting the nucleocytoplasmic volume ratio. J Cell Biol 115:941–948

37. Chene P (2000) Fast, qualitative analysis of p53 phosphorylation by protein kinases. Biotechniques 28:240–242
38. Sheng Y, Laister RC, Lemak A, Wu B, Tai E, Duan S, Lukin J, Sunnerhagen M, Srisailam S, Karra M, Benchimol S, Arrowsmith CH (2008) Molecular basis of Pirh2-mediated p53 ubiquitylation. Nat Struct Mol Biol 15:1334–1342
39. Nie Y, Li HH, Bula CM, Liu X (2000) Stimulation of p53 DNA binding by c-Abl requires the p53 C terminus and tetramerization. Mol Cell Biol 20:741–748
40. Foo RSY, Nam YJ, Ostreicher MJ, Metzl MD, Whelan RS, Peng CF, Ashton AW, Fu W, Mani K, Chin SF, Provenzano E, Ellis I, Figg N, Pinder S, Bennett MR, Caldas C, Kitsis RN (2007) Regulation of p53 tetramerization and nuclear export by ARC. Proc Natl Acad Sci USA 104:20826–20831
41. van Dieck J, Fernandez–Fernandez MR, Veprintsev DB, Fersht AR (2009) Modulation of the oligomerization state of p53 by differential binding of proteins of the S100 family to p53 monomers and tetramers. J Biol Chem 284:13804–13811
42. Rajagopalan S, Jaulent AM, Wells M, Veprintsev DB, Fersht AR (2008) 14-3-3 activation of DNA binding of p53 by enhancing its association into tetramers. Nucleic Acids Res 36: 5983–5991
43. Soussi T, Kato S, Levy PP, Ishioka C (2005) Reassessment of the TP53 mutation database in human disease by data mining with a library of TP53 missense mutations. Hum Mutat 25:6–17
44. Miller M, Lubkowski J, Rao JKM, Danishefsky AT, Omichinski JG, Sakaguchi K, Sakamoto H, Appella E, Gronenborn AM, Clore GM (1996) The oligomerization domain of p53: crystal structure of the trigonal form. FEBS Lett 399:166–170
45. Merritt J, Roberts KG, Butz JA, Edwards JS (2007) Parallel analysis of tetramerization domain mutants of the human p53 protein using PCR colonies. Genomic Med 1:113–124
46. Whibley C, Pharoah PD, Hollstein M (2009) p53 polymorphisms: cancer implications. Nat Rev Cancer 9:95–107
47. Feng L, Hollstein M, Xu Y (2006) Ser46 phosphorylation regulates p53-dependent apoptosis and replicative senescence. Cell Cycle 5:2812–2819
48. Mantovani F, Tocco F, Girardini J, Smith P, Gasco M, Lu X, Crook T, Del Sal G (2007) The prolyl isomerase Pin1 orchestrates p53 acetylation and dissociation from the apoptosis inhibitor iASPP. Nat Struct Mol Biol 14:912–920
49. Bergamaschi D, Samuels Y, Sullivan A, Zvelebil M, Breyssens H, Bisso A, Del Sal G, Syed N, Smith P, Gasco M, Crook T, Lu X (2006) iASPP preferentially binds p53 proline-rich region and modulates apoptotic function of codon 72-polymorphic p53. Nat Genet 38:1133–1141
50. Bond GL, Hu W, Bond EE, Robins H, Lutzker SG, Arva NC, Bargonetti J, Bartel F, Taubert H, Wuerl P, Onel K, Yip L, Hwang SJ, Strong LC, Lozano G, Levine AJ (2004) A single nucleotide polymorphism in the MDM2 promoter attenuates the p53 tumor suppressor pathway and accelerates tumor formation in humans. Cell 119:591–602
51. Kamada R, Nomura T, Anderson CW, Sakaguchi K (2011) Cancer-associated p53 tetramerization domain mutants: quantitative analysis reveals a low threshold for tumor suppressor inactivation. J Biol Chem 286:252–258